Macromolecular Research

Article

DOI 10.1007/s13233-018-6062-8

www.springer.com/13233 pISSN 1598-5032 eISSN 2092-7673

High-Efficiency Flexible and Foldable Paper-Based Supercapacitors Using Water-Dispersible Polyaniline-Poly(2-acrylamido-2-methyl-1-propanesulfonic acid) and Poly(vinyl alcohol) as Conducting Agent and Polymer Matrix

Seung Won Kang
Joonho Bae*

Department of Nano-physics, Gachon University, Seongnam, Gyeonggi 13120, Korea

Received Frbruary 25, 2017 / Revised October 16, 2017 / Accepted December 25, 2017

Abstract: For the first time, common printing paper is converted to electrode for high-performance flexible and foldable electrochemical supercapacitor using water-dispersible conductive polymer, polyaniline-poly(2-acrylamido-2-methyl-1-propanesulfonic acid) (PANI-PAAMPSA) and poly(vinyl alcohol) (PVA) as conducting agent and polymer matrix, respectively. PANI-PAAMPSA is used to convert insulating paper to conductive substrate while PVA provides ion channels for electrolyte as well as mechanical durability for paper substrate. The paper-based supercapacitors exhibit excellent electrochemical energy storage capability. The maximum mass and area specific capacitances of the paper-based supercapacitors reached up to 41 F g^{-1} and 45 mF cm^{-2} at 20 mV s^{-1}, respectively. In addition, the PANI-PAAMPSA/PVA/paper-based supercapacitors demonstrate high mechanical durability and flexibility during the bending tests. The specific capacitance of the paper-based supercapacitors are changed up to 16 % compared to the initial value as they are bent progressively from 0° to 100°. The excellent electrochemical stability of the paper-based supercapacitors is attributed to high water dispersibility and conductivity of PANI-PAAMPSA. The high mechanical durability is attributed to employment of PVA as robust polymer matrix allowing for ion channels of electrolyte. Our work can open up opportunities of next-generation paper-based electronics and energy storage devices.

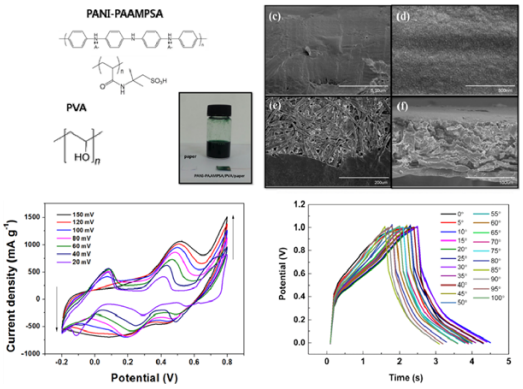

Keywords: polyaniline-poly(2-acrylamido-2-methyl-1-propanesulfonic acid), poly(vinyl alcohol), paper, supercapacitor, energy storage devices.

1. Introduction

Recently, paper has attracted significant interest as novel and flexible substrate.[1-3] Papers are composed of cellulose fibers with versatile properties such as flexibility, lightweightness, and foldability.[1] Paper can be produced from raw materials which are earth-abundant and renewable, making it one of the cheapest flexible substrates. Furthermore, the printing technology is fully established to facilitate the next-generation paper-based electronics.

There has been steady progress in employing papers as novel flexible substrates for electronic devices including microfluidics,[4] thin film transistors,[5] printed electronics,[6,7] and conductive papers.[8,9] One of the most promising applications of paper substrates is the electrodes for the energy storage device. Due to the development of flexible and wearable personal electronics, novel flexible and efficient electrode materials of energy storage devices are becoming increasingly important. The integrated flexible energy storage systems are necessary to fully utilize the flexible electronics. The conductive papers possess high flexibility as well as electrical conductivity. Papers have highly porous structure due to the networks of the cellulose fibers. The flexibility of papers could overcome the mechanical cracking and failure of the tin indium oxide (ITO) film, which is the conventional transparent electrode. The high porosity of papers enables sufficient surface area required for the flexible electrodes of lithium ion batteries and electrochemical capacitors or supercapacitors which are the state-of-the-art energy storage devices.

To realize paper-based electronics or energy devices, several technical issues need to be resolved. Firstly, common printing papers made of cellulose fibers have weak adhesion to metal films which are critical to make papers conductive.[10] Secondly, papers tear easily, indicating that their mechanical durability needs to be significantly improved for paper-based devices.

Herein, we report high efficiency flexible and foldable supercapacitors on paper substrates using polyaniline-poly(2-acrylamido-2-methyl-1-propanesulfonic acid) (PANI-PAAMPSA) mixed

Acknowledgments: This work was supported by the Technology Innovation Program (10052774, Development of hybrid supercapacitor by nano structure carbon for ISG Applications) funded by the Ministry of Trade, Industry & Energy (MI, Korea). This research was supported by Basic Science Research Program through the National Research Foundation of Korea (NRF) funded by the Ministry of Science, ICT & Future Planning (2017R1D1A1B03032466).

***Corresponding Author:** Joonho Bae (baejh2k@gachon.ac.kr)

with polyvinyl alcohol (PVA) as electrode materials. The PANI-PAAMPSA and PVA-based supercapacitors overcome the two obstacles mentioned above. Common printing papers are converted successfully to conductive substrates without use of any metal coatings. Due to its high water solubility and conductivity, PANI-PAAMPSA is deposited effectively, making papers conductive enough to be used as electrodes for supercapacitors. The PVA admixed with PANI-PAAMPSA plays a role of the polymer matrix to allow for ion conduction in PANI-PAAMPSA while significantly enhancing the mechanical stability of paper substrates.

2. Experimental

2.1. Synthesis of PANI-PAAMPSA

To synthesize the water soluble conductive polymer, PANI-PAAMPSA, poly(2-acrylamido-2-methyl-1-propanesulfonic acid) or PAAMPSA (Aldrich, MW : 800,000) was dissolved in deionized water. PAAMPSA solution was mixed with aniline monomer (Aldrich) and stirred at room temperature for 30 min. Ammonium persulfate (98%, Aldrich) used as an oxidizing agent was dissolved in deionized water and stirred for 30 min. The ammonium persulfate solution was added dropwise to the PAAMPSA-aniline solution. The reaction medium of Ammonium persulfate and PAAMPSA-aniline solution was kept at ice-water temperature for 6 h and subsequently at room temperature overnight. Finally, the polymer suspension of PANI-PAAMPSA was precipitated by acetone.

2.2. Preparation of PANI-PAAMPSA/PVA solution and paper electrodes

The PANI-PAAMPSA in a powder form was dissolved in deionized water at 2.4 wt%. To admix the PANI-PAAMPSA with PVA, PVA (99%, Aldrich) was added to the aqueous solution of PANI-PAAMPSA and ultra-sonicated for 30 min. The common printing papers were drop coated with the PANI-PAAMPSA/PVA solution.

2.3. Materials characterization

The surface morphology of the paper electrodes hybridized with PANI-PAAMPSA and PVA was investigated by using field emission scanning electron microscopy (SEM) (JEOL) at the acceleration voltage of 10 kV. The exposed (measurement) area of the electrode ranged from ~660×660 nm^2 to ~350×350 um^2 depending on the magnification. For the cross-section SEM measurements of the paper electrodes, the electrodes were cleaved with a razor knife, and SEM images of their cross section were taken. The thickness of the electrode was measured to be ~126 μm. The X-ray photoelectron spectroscopy (XPS) measurements were performed on the paper electrodes using a Quantera SXM. The maximum energy resolution of XPS was 0.5 eV. The weights of the electrode material were measured using a microbalance (Mettler Toledo). The size of the electrodes is typically 1 cm^2.

2.4. Electrochemical measurement of the paper-based supercapacitors

The cyclic voltammetry (CV), galvanostatic charge-discharge, and electrochemical impedance spectroscopy (EIS) measurements on PANI-PAAMPSA/PVA/paper electrode were performed in a three-electrode configuration using 2 M H_2SO_4 aqueous solution as electrolyte. The electrolyte was prepared by diluting the concentration of sulfuric acid (98%, Daejung, Korea). The as-prepared PANI-PAAMPSA/PVA/paper electrode, Ag/AgCl electrode and Pt foil or wire were used as the working, reference, and counter electrode, respectively. The bending tests were conducted on the paper-based supercapacitors in two electrode configuration. A glass fiber filter (Whatman, GE) was used as the separator. The bending angle ranged from 0° to 100° with the step of 5°. Electrochemical characteristics of the supercapacitors were measured by potentiostat (Versastat 4). All the electrochemical measurements were conducted at the room temperature.

3. Results and discussion

3.1. Material characterizations of paper coated with PANI-PAAMPSA/PVA

The chemical structures of PANI-PAAMPSA and PVA are shown in Figure 1(a). PANI-PAAMPSA is the electrically conductive emeraldine salt forms of PANI doped with the excess pendant sulfonic acid groups from PAAMPSA to enable its water dispersibility.[11] PVA is a well-known polymer with high water-absorbing and holding capacity, high gel strength and low cost.[12] PVA plays a role of the polymer matrix for PANI-PAAMPSA. The PVA polymer matrix provides two capabilities for PANI-PAAMPSA conducting agents of papers. Firstly, PVA allows for effective ion channels for mobile ions of the electrolytes, which is the reason for its being used main polymer matrix of gel electrolytes in supercapacitors.[13,14] PVA also can dramatically enhance mechanical strength of conducting polymer films or papers. It is reported that PANI embedded in PVA polymer matrix significantly enhances the mechanical strength and adhesion of the PANI film.[15] Figure 1(b) shows a photo of aqueous solution of PANI-PAAMPSA mixed with PVA. The dark green PANI-PAAMPSA solution is shown to be uniformly dispersed in water. When the PANI-PAAMPSA solution was mixed with PVA, the uniformity of dispersion did not change from that of PANI-PAAMPSA solution. The paper electrode fabricated by dip coating of common printing paper and original paper are also shown in Figure 1(b). The white paper is transformed to flexible and porous electrodes. The change of color (from white to dark green) is noticeable.

Figure 1(c) and (d) show the surface morphology of the paper hybridized with PANI-PAAMPSA and PVA. Each SEM image shows a uniform coating of the conductive polymer on the paper. Cross sectional SEM image of a PANI-PAAMPSA/PVA/paper electrode is shown Figure 1(f). The networks of the cellulose fiber as seen in Figure 1(e) are not seen anymore. The aggregation of polymers suggests that the cellulose fibers are covered or coated by the conductive polymer (PANI-PAAMPSA) embedded in polymer matrix (PVA). This image also indicates that the whole vol-

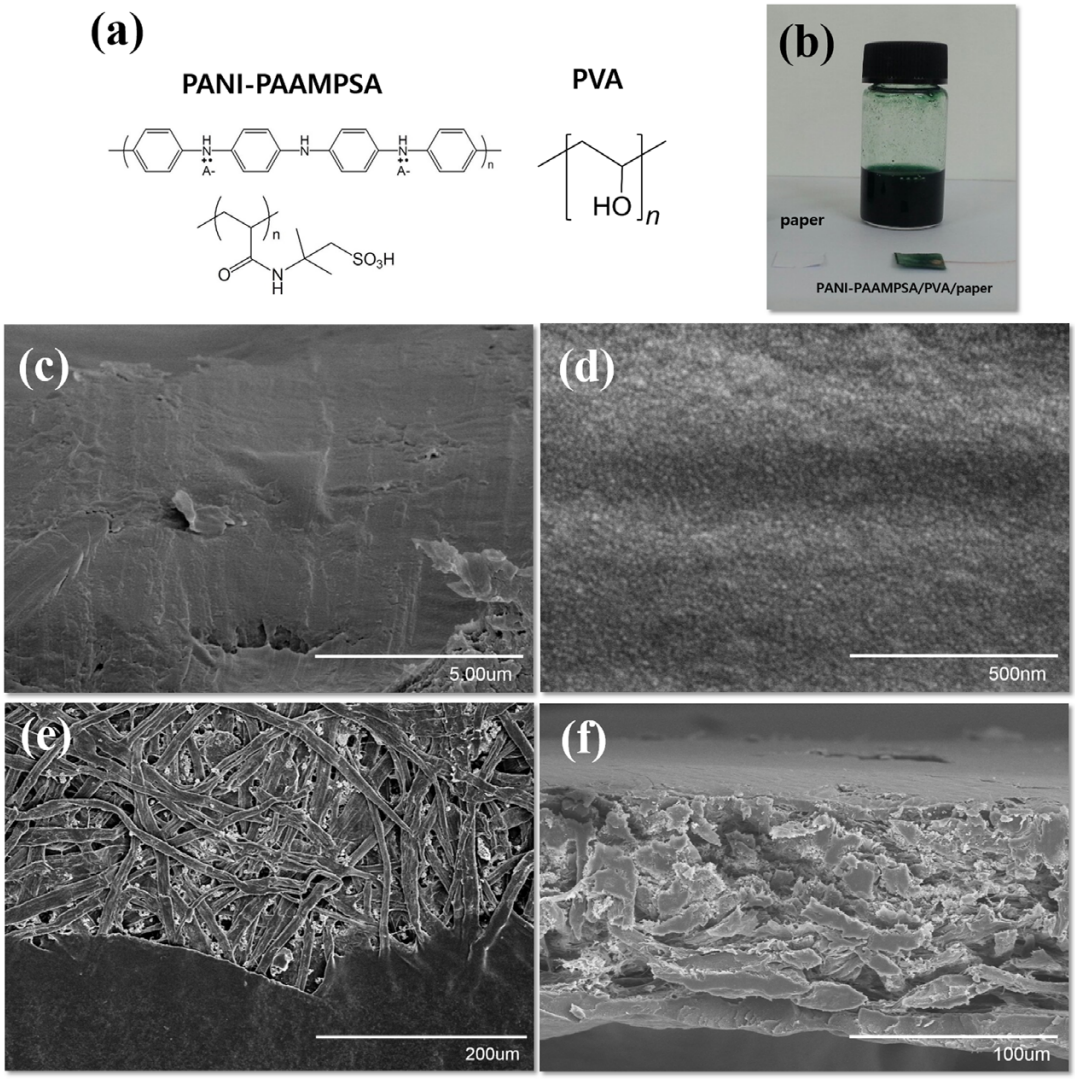

Figure 1. (a) Chemical structure of PANI-PAAMPSA and PVA. (b) Photo of PANI-PAAMPSA/PVA mixture dissolved in water, bare printing paper, and PANI-PAAMPSA/paper substrate. (c)-(e) SEM images of PANI-PAAMPSA/PVA/paper substrate. (f) Cross-sectional SEM image of PANI-PAAMPSA/PVA/paper substrate.

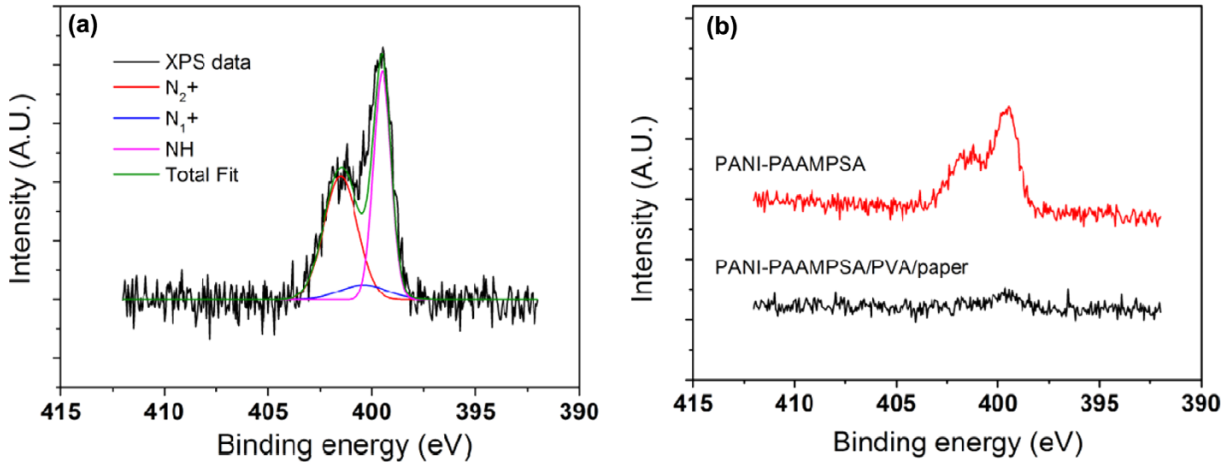

Figure 2. (a) High resolution XPS spectra of as-prepared PANI-PAAMPSA powder. (b) XPS spectra near the nitrogen (1s level) of as-prepared PANI-PAAMPSA powder and PANI-PAAMPSA/PVA/paper substrate.

ume inside the paper is fully hybridized with PANI-PAAMPSA and PVA.

The XPS measurements were also carried out to confirm successful synthesis of PANI-PAAMPSA. Figure 2(b) shows the XPS spectrum near the nitrogen (1s level) in as-prepared PANI-PAAMPSA in powder form. Conventionally, this N1s peak is

deconvoluted into three components with the Gaussian functions using the non-linear least square analysis.[16] A peak located at 399.50 eV resulted from the amide groups (denoted as NH) in PAAMPSA. There are two peaks associated with the protonated nitrogens. One peak at 400.40 eV (N_1^+) corresponds to protonated nitrogens associated with polarons and bipolarons in the conducting polymer. The peak centered at 401.50 eV (N_2^+) is attributed to the sulfonic acid groups in PAAMPSA. This result confirms the successful synthesis of PANI-PAAMPSA.

The XPS measurements were also performed on the paper electrode hybridized with PANI-PAAMPSA and PVA. It is seen that the XPS spectrum near the nitrogen (1s level) from PANI-PAAMPSA/PVA/paper resulted in significantly lower intensity than that from as-prepared PANI-PAAMPSA powder. The lowered intensity indicates the relative content of PANI-PAAMPSA in PANI-PAAMPSA/PVA mixture is reduced due to the content of PVA. Since the content of PANI-PAAMPSA affects the conductivity of PANI-PAAMPSA/PVA/paper electrodes, the conductivity of the electrodes can be controlled and optimized by varying the relative concentration of PANI-PAAMPSA in PANI-PAAMPSA/PVA mixture. This XPS observation suggests that characteristics of PANI-PAAMPSA/PVA/paper –based supercapacitor can be further enhanced by controlling the PANI-PAAMPSA concentration.

3.2. Electrochemical characteristics of PANI-PAAMPSA/PVA/paper-based supercapacitors

To explore the possibility of PANI-PAAMPSA/PVA/paper electrodes in electrochemical applications, cyclic voltammetry (CV) tests were performed. Figure 3(a) shows the resultant CV curves obtained from a PANI-PAAMPSA/PVA/paper electrode in 2 M H_2SO_4 (aq) electrolyte. The voltage range is -0.2–0.8 V and the scan rates are 150, 120, 100, 80, 60, 40, and 20 mV s^{-1}. The CV curves exhibit the redox peaks, suggesting the pseudocapacitve behavior of the PANI-PAAMPSA/PVA/paper electrodes. In addition, the mass-specific current densities increased with increased scan rates, indicating the typical rate capability of supercapacitors. The CV curve measured at a scan rate of 100 mV s^{-1} is redrawn in Figure 2(b). It is clearly seen that the oxidation and reduction peak appear within approximately 0 to 0.5 V. Similar redox peaks were reported in previous work on electrochemistry of PANI-PAAMPSA electrodes in acetate buffer solution.[17] It was reported that the redox peaks were attributed to the transitions between the pernigraniline/leucoemeraldine base state to the emeraldine form.[17] Since our supercapacitors employed regular paper without prior cleaning and PVA besides PANI-PAAMPSA, it is not clear the peaks originate totally from PANI-PAAMPSA or other chemical species are playing role or not.

The CV results above can be employed to determine the spe-

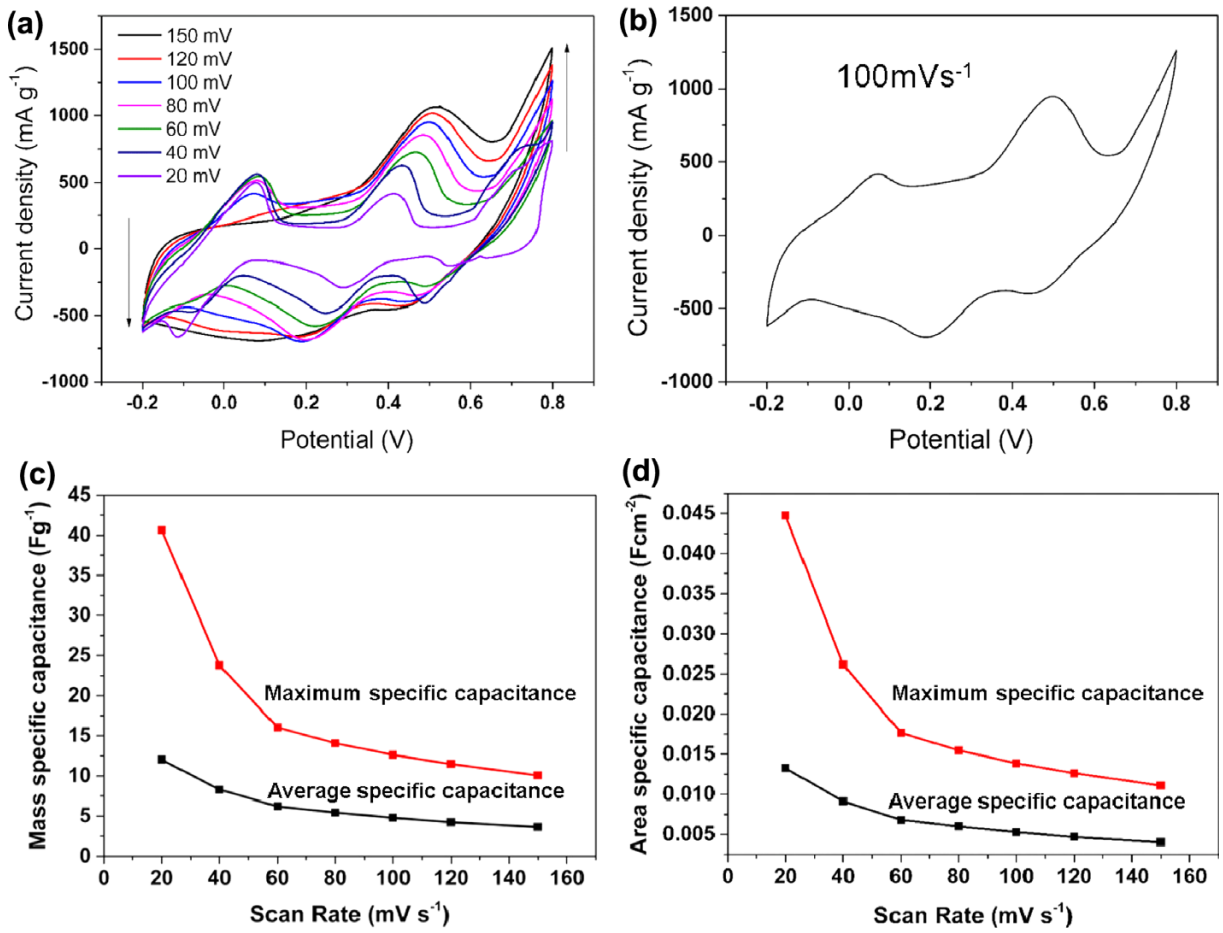

Figure 3. (a) CV curves of PANI-PAAMPSA/PVA/paper-based supercapacitor using 2 M H_2SO_4 as an electrolyte. The scan rates are 20-150 mV s^{-1}. (b) CV curve at 100 mV s^{-1} shown in (a). (c) The mass specific capacitance (C_M) obtained from the CV curve in (a). (d) The area specific capacitance (C_A) obtained from the CV curve in (a).

cific capacitances of the supercapacitors according to $C_M=I\cdot S^{-1}\cdot M^{-1}$ or $C_A=I\cdot S^{-1}\cdot A^{-1}$, where C_M (C_A) is the mass (area) specific capacitance, I is the corresponding current at the voltage applied.[18] The maximum specific capacitances (C_M and C_A) of the PANI-PAAMPSA/paper-based supercapacitors obtained by using these equations are depicted in Figure 3(c) and (d). The plots show that the capacitances increase with the decreased scan rates, which is the limited rate performance of the supercapacitors. It is reported that the possible reason for this rate performance is the inhomogeneous porosity of the electrodes.[19] The mass and area specific capacitances reached up to 41 F g^{-1} and 45 mF cm^{-2} at 20 mV s^{-1}, respectively.

Since the CV curves are not rectangular, the following equations can be used to calculate the average mass and area specific capacitances:

$$C_M = \frac{1}{MS(V_2-V_1)}\int_{V_1}^{V_2} IdV \quad (1)$$

$$C_A = \frac{1}{AS(V_2-V_1)}\int_{V_1}^{V_2} IdV \quad (2)$$

where C_M is the mass specific capacitance, C_A is the area specific capacitance, M is the mass of the active materials (PANI-PAAMPSAs), A is the area of the electrode, S is the scan rate, V_1 and V_2 are the lower and upper limit of the potential range, and I is the current in the CV curves.

The average specific capacitances are also shown in Figure 2(c) and (d). Again the highest capacitances are obtained at the lowest scan rate of 20 mV s^{-1} as shown in the curves of average specific capacitances vs. scan rates. At 20 mV s^{-1}, the average mass and area specific capacitances are 12 F g^{-1} and 13 mF cm^{-2}, respectively.

Herein, it is noteworthy to discuss and compare the specific capacitances of our PANI-PAAMPSA/PVA/paper-based supercapacitors with other reports in literature. Since the first report on the synthesis of PANI-PAAMPSA is recent, the works on the electrochemistry or electrochemical energy devices employing PANI-PAAMPSA as electrodes are limited. Probably, we can compare the specific capacitances of the PANI-PAAMPSA/PVA/paper electrodes with those from PANI electrodes in literature. The maximum and average C_M values discussed above are comparable to ones obtained from PANI-based supercapacitors. Various PANI-based supercapacitors in various electrolytes are reported to demonstrate the mass specific capacitances of 5-107 F g^{-1}.[20-22] The specific capacitances of PANI-PAAMPSA/PVA/paper-based supercapacitors could be further increased by engineering the surface structure of the electrode to increase the surface area as reported in graphene-based supercapacitors.[23,24]

The electrochemical properties of PANI-PAAMPSA/PVA/paper-based supercapacitors were further characterized by the galvanostatic charge-discharge tests. The resultant charge-discharge curves at the current densities of 1, 2, and 4 A g^{-1} are shown in Figure 4(a). The specific capacitances (C_M and C_A) can be also obtained from the charge-discharge curves using $C_M=I\Delta t\cdot(M\Delta V)^{-1}$, where I is the discharge current, Δt is the discharge time, M is the mass of active material of electrode, and ΔV is the potential window. The mass specific capacitances of PANI-PAAMPSA/paper-based supercapacitors determined from charge-discharge curves at the current densities of 1, 2, and 4 A g^{-1} (Figure 4(a)) are 5.1, 4.4, and 2.8 F g^{-1}, respectively.

To further characterize the electrochemical performances of the PANI-PAAMPSA/PVA/paper-based electrodes, the EIS measurements were carried out in the same 2 M H_2SO_4 (aq) electrolyte. Figure 4(b) shows the Nyquist plot from EIS data in the frequency range of 1 MHz to 125 mHz. The applied potential was 10 mV RMS. The Nyquist plot shows two distinct parts of a semicircle in the high frequency region and a line in the low frequency region. In literature, the intersection point on the x axis at high frequency is defined as the internal resistance or R_s of supercapacitor electrodes, which determines the operation rates of a capacitor or power capability.[25,26]

The diameter of the semicircle originated from the charge transfer resistance on the electrode surface (R_{ct}).[27,28] An EIS simulation tool was employed to determine R_s and R_{ct} by fitting the experimental data in Figure 4(b) (Supplementary information). The R_s value of PANI-PAAMPSA/PVA/paper-based supercapacitors,

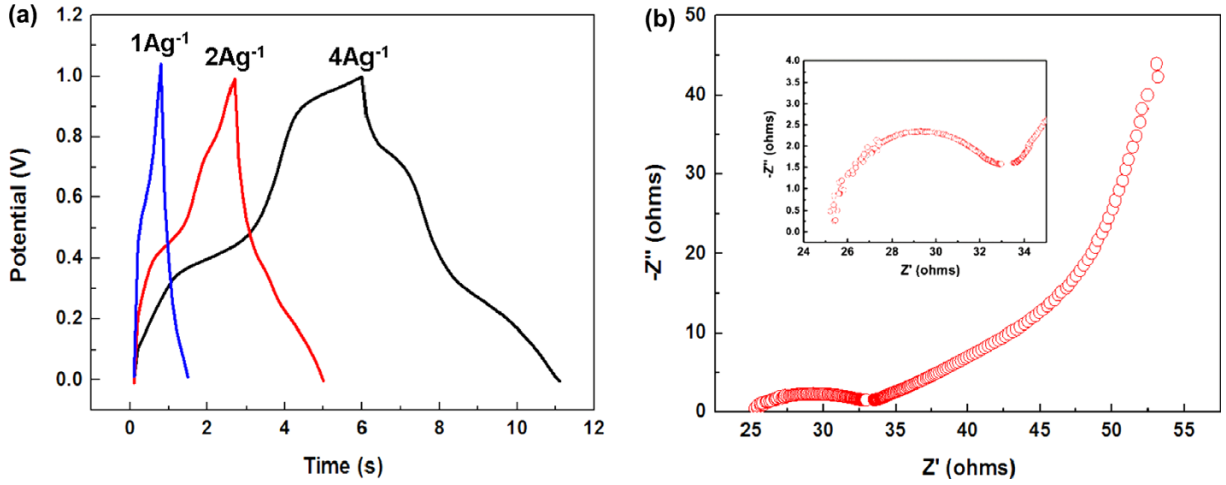

Figure 4. (a) Galvanostatic charge-discharge curves of PANI-PAAMPSA/PVA/paper-based supercapacitor using 2 M H_2SO_4 electrolyte. The charge densities are 1, 2, and 4 A g^{-1}. (b) EIS result (Nyquist plot) from the PANI-PAAMPSA/PVA/paper-based supercapacitor. The inset: a magnified view of the high frequency region of the impedance spectra.

which is defined by the intersection point on the x axis, is 25 Ω. This value of R_s or the internal resistance is comparable to those of supercapacitors in literature. The carbon nanotube-based supercapacitors are reported to exhibit the internal resistances of 0.5~500 Ω in various electrolytes.[29,30] The R_{ct} value was determined to be 9.2 Ω. In the equivalent circuit, the charge transfer resistance is placed in parallel being responsible for the self-discharge of the capacitors.[31,32] Since the projected area of the paper electrode is 1 cm^2, the normalized R_s and R_{ct} can be expressed as 25 and 9.2 Ω cm^{-2}. It is also seen that the Nyquist plot demonstrates the change in slope in the low frequency region, suggesting the ionic diffusion limitation or different diffusion process in various pores in electrodes, as observed in various supercapacitors in literature.[21,33-37] For instance, two regimes of 45° line and an almost vertical line were observed during the EIS measurements of single walled carbon nanotubes.[36,37] The change in the slope was attributed to the diffusion through the pores of different electrode materials (bucky-paper and nanotubes). Similarly, the change in the slope in our paper-based supercapacitors could be attributed to the different diffusion process in various pores in the electrodes. The observation on the EIS results indicates that the paper with PANI-PAAMPSA is a promising supercapacitor electrode.

As mentioned above, one of the limitations of papers for flexible substrates is their low mechanical durability. We adopted PVA to significantly enhance mechanical stability of paper substrates. PVA gel impregnating papers provides the resistance to being torn apart. Furthermore, PVA enables sufficient ion channels for electrolytes as shown in PVA gel electrolytes for supercapacitors. To test mechanical stability and flexibility of the PANI-PAAMPSA/paper supercapacitors, mechanical bending test was conducted. The supercapacitor was bent at the angle which increased progressively from 0° to 100° at the step of 5°. The charge-discharge tests were performed at each bending angles (Figure 5(a)). It is seen that the distinct triangular charge-discharge curves appear at all angles. Using the discharge times in each charge-discharge test, the ratio (C/C_0) of capacitance (C) to initial capacitance (C_0) can be calculated at each angle (Figure 5(b)). Compared to the initial angle (0°), the capacitance increases until the bending angle reaches up to 10°. The maximum increase of the specific capacitance is 16 % at 10°. After the bending angle of 10°, the capacitance is found to gradually decrease. The increase of the capacitance at the early range of bending angle (5°-10°) may have been caused by increase of pressure on the electrodes, resulting in the enhancement of electrolyte transport in the glass fiber filter. At the maximum bending angle of 100°, the specific capacitance is 89%. The capacitance change is 11% compared to the original capacitance (C_0). These results indicate that the specific capacitance of PANI-PAAMPSA/paper supercapacitor showed the maximum change of 16% up to the bending angle of 100°. The high mechanical durability is attributed to employment of PVA as polymer matrix allowing for ion channels of electrolyte and enhancement of mechanical durability.

4. Conclusions

In summary, common printing paper was converted to electrode for high-performance flexible and foldable electrochemical capacitors using the conducting agent and polymer matrix. The water-dispersible conductive polymer PANI-PAAMPSA and PVA were employed as the conducting agent and the polymer matrix, respectively. By depositing PANI-PAAMPSA and PVA mixture on papers, PANI-PAAMPSA effectively transformed the insulating papers into conductive electrodes. PVA gel in the mixture hardened the paper substrate to enhance the mechanical stability of paper substrates while providing sufficient ion channels for electrolyte ions. The paper-based supercapacitors exhibit excellent electrochemical energy storage capability as evidenced by the high maximum mass (41 F g^{-1}) and area specific capacitances (45 mF cm^{-2}) at 20 mV s^{-1}. PANI-PAAMPSA/PVA/paper-based supercapacitors also demonstrated high mechanical durability and flexibility during the bending tests. The excellent electrochemical characteristics are attributed to high water dispersibility and conductivity of PANI-PAAMPSA, which converts the insulating papers into conductive substrates effectively. The use of PVA enabled sufficient ion channels of electrolyte ions and enhancement of mechanical durability of entire PANI-PAAMPSA/PVA/paper substrate. The overall electrochemical and mechanical properties can be further enhanced by optimizing PANI-PAAMPSA content in PANI-PAAMPSA/PVA/paper substrate. The results indicated that

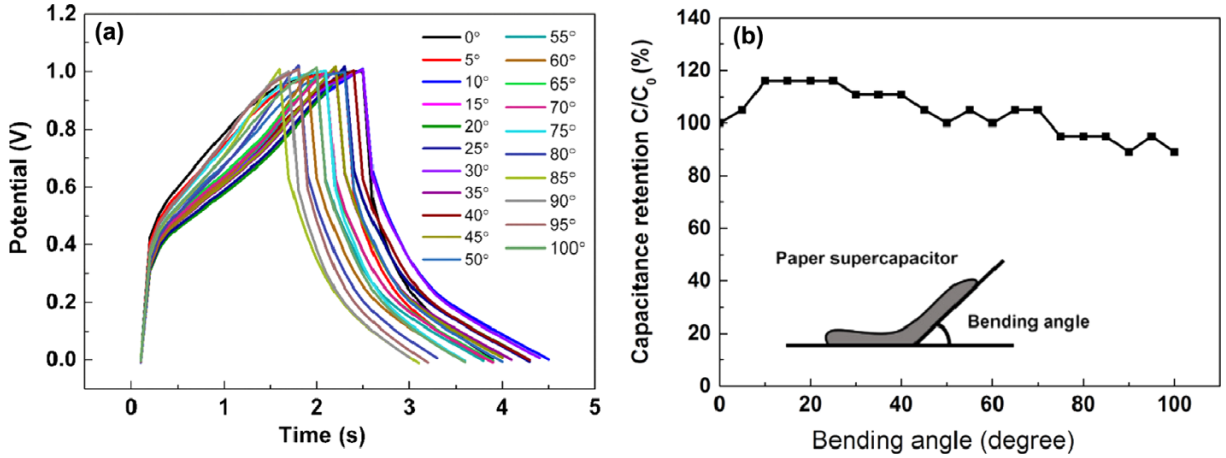

Figure 5. The result of the mechanical bending test performed on PANI-PAAMPSA/PVA/paper-based supercapacitor. The inset shows an illustration to define the bending angles.

our strategy could help us to realize highly efficient paper-based conductive substrates for next-generation paper-based electronics and energy storage devices.

Supporting information: Information is available regarding the conductivity measurements of paper electrodes and the EIS fitting. The materials are available *via* the Internet at http://www.springer.com/13233.

References

(1) L. B. Hu and Y. Cui, *Energy Environ. Sci.*, **5**, 6423 (2012).
(2) Y. J. Kang, H. Chung, C. H. Han, and W. Kim, *Nanotechnology*, **23**, 065401 (2012).
(3) P. Andersson, D. Nilsson, P.O. Svensson, M. Chen, A. Malmström, T. Remonen, T. Kugler, and M. Berggren, *Adv. Mater.*, **14**, 1460 (2002).
(4) A. W. Martinez, S. T. Phillips, M. J. Butte, and G. M. Whitesides, *Angew. Chem. Int. Ed.*, **46**, 1318 (2007).
(5) F. Eder, H. Klauk, M. Halik, U. Zschieschang, G. Schmid, and C. Dehm, *Appl. Phys. Lett.*, **84**, 2673 (2004).
(6) P. Andersson, D. Nilsson, P.-O. Svensson, M. Chen, A. Malmström, T. Remonen, T. Kugler, and M. Berggren, *Adv. Mater.*, **14**, 1460 (2002).
(7) Y.-H. Kim, D.-G. Moon, and J.-I. Han, *IEEE Electron Device Lett.*, **25**, 702 (2004).
(8) L. Wang, W. Chen, D. Xu, B. S. Shim, Y. Zhu, F. Sun, L. Liu, C. Peng, Z. Jin, and C. Xu, *Nano Lett.*, **9**, 4147 (2009).
(9) L. Hu, J.W. Choi, Y. Yang, S. Jeong, F. La Mantia, L.-F. Cui, and Y. Cui, *Proc. Natl. Acad. Sci. U.S.A.*, **106**, 21490 (2009).
(10) L. Y. Yuan, X. Xiao, T. P. Ding, J. W. Zhong, X. H. Zhang, Y. Shen, B. Hu, Y. H. Huang, J. Zhou, and Z. L. Wang, *Angew. Chem. Int. Ed.*, **51**, 4934 (2012).
(11) J. E. Yoo, J. L. Cross, T. L. Bucholz, K. S. Lee, M. P. Espe, and Y.-L. Loo, *J. Mater. Chem.*, **17**, 1268 (2007).
(12) G. Q. Zhang and X. G. Zhang, *Solid State Ionics*, **160**, 155 (2003).
(13) H. Gao and K. Lian, *J. Power Sources*, **196**, 8855 (2011).
(14) J. Y. Kim, C. S. Lee, J. H. Han, J. W. Cho, and J. Bae, *Electrochem. Solid-State Lett.*, **14**, A56 (2011).
(15) D. S. Patil, J. S. Shaikh, D. S. Dalavi, S. S. Kalagi, and P. S. Patil, *Mater. Chem. Phys.*, **128**, 449 (2011).
(16) J. E. Yoo, *Understanding the Processing-Structure-Property Relationships of Water-Dispersible, Conductive Polyaniline*, in *Chemical Engineering*, the University of Texas at Austin, the University of Texas at Austin, Ph. D. Dissertation, 2009, p 250.
(17) J. Tarver, J. E. Yoo, T. J. Dennes, J. Schwartz, and Y.-L. Loo, *Chem. Mater.*, **21**, 280 (2008).
(18) M. Kaempgen, J. Ma, G. Gruner, G. Wee, and S. G. Mhaisalkar, *Appl. Phys. Lett.*, **90**, 264104 (2007).
(19) Y. Yoon, K. Lee, C. Baik, H. Yoo, M. Min, Y. Park, S. M. Lee, and H. Lee, *Adv. Mater.*, **25**, 4437 (2013).
(20) K. S. Ryu, Y. Lee, K.-S. Han, Y. J. Park, M. G. Kang, N.-G. Park, and S. H. Chang, *Solid State Ionics*, **175**, 765 (2004).
(21) K. S. Ryu, K. M. Kim, N.-G. Park, Y. J. Park, and S. H. Chang, *J. Power Sources*, **103**, 305 (2002).
(22) W.-C. Chen, T.-C. Wen, and H. Teng, *Electrochim. Acta*, **48**, 641 (2003).
(23) L. Zhang and G. Shi, *J. Phys. Chem.*, **115**, 17206 (2011).
(24) C. M. Chen, Q. Zhang, C. H. Huang, X. C. Zhao, B. S. Zhang, Q. Q. Kong, M. Z. Wang, Y. G. Yang, R. Cai, and D. Sheng Su, *Chem. Commun. (Camb)*, **48**, 7149 (2012).
(25) X. Yang, J. Zhu, L. Qiu, and D. Li, *Adv. Mater.*, **23**, 2833 (2011).
(26) Y. Luo, J. Jiang, W. Zhou, H. Yang, J. Luo, X. Qi, H. Zhang, Y. Denis, C. M. Li, and T. Yu, *J. Mater. Chem.*, **22**, 8634 (2012).
(27) X. Zhang, X. Wang, L. Jiang, H. Wu, C. Wu, and J. Su, *J. Power Sources*, **216**, 290 (2012).
(28) S. Peng, L. Li, H. Tan, R. Cai, W. Shi, C. Li, S.G. Mhaisalkar, M. Srinivasan, S. Ramakrishna, and Q. Yan, *Adv. Funct. Mater.*, **24**, 2155 (2014).
(29) M. Kaempgen, C. K. Chan, J. Ma, Y. Cui, and G. Gruner, *Nano Lett.*, **9**, 1872 (2009).
(30) B. Dong, B.-L. He, C.-L. Xu, and H.-L. Li, *Mater. Sci. Eng. B: Adv.*, **143**, 7 (2007).
(31) E. Frackowiak, K. Metenier, V. Bertagna, and F. Beguin, *Appl. Phys. Lett.*, **77**, 2421 (2000).
(32) H. Niu, D. Zhou, X. Yang, X. Li, Q. Wang, and F. Qu, *J. Mater. Chem. A*, **3**, 18413 (2015).
(33) Q. Cheng, J. Tang, J. Ma, H. Zhang, N. Shinya, and L.-C. Qin, *Phys. Chem. Chem. Phys.*, **13**, 17615 (2011).
(34) M. D. Stoller, S. Park, Y. Zhu, J. An, and R. S. Ruoff, *Nano Lett.*, **8**, 3498 (2008).
(35) Y. Chen, X. Zhang, D. Zhang, P. Yu, and Y. Ma, *Carbon*, **49**, 573 (2011).
(36) A. Claye, J. E. Fischer, and A. Métrot, *Chem. Phys. Lett.*, **330**, 61 (2000).
(37) S. Ng, J. Wang, Z. Guo, J. Chen, G. Wang, and H. K. Liu, *Electrochim. Acta*, **51**, 23 (2005).